Journal of Materials Science: Materials in Electronics (2020) 31:10478–10488
https://doi.org/10.1007/s10854-020-03596-0

Optical properties and electronic structure of V_2O_5, V_2O_3 and VO_2

Krystyna Schneider[1]

Received: 16 March 2020 / Accepted: 12 May 2020 / Published online: 22 May 2020
© The Author(s) 2020

Abstract
The electronic structure of the three main vanadium oxides—V_2O_3, VO_2 and V_2O_5—is reviewed. The optical properties of vanadium pentoxide thin films were determined. It was found that a direct allowed transition is the most probable one in the studied vanadium pentoxide thin films.

Abbreviations

APW	Augmented-plane wave
CB	Conduction band
DA	Direct allowed
DF	Direct forbidden
DFT	Density function theory
E_F	Fermi energy
E_g	Energy gap
ELS	Electron energy loss
IA	Indirect allowed
IF	Indirect forbidden
MIT	Metal–insulator transmission
PES	Photoemission spectroscopy
PL	Photoluminescence
SXS	Soft X-ray spectroscopy
T.F.	Thin film
VB	Valence band
XAS	X-ray adsorption spectroscopy
XES	X-ray emission spectroscopy
XPS	X-ray photoelectron spectroscopy
XRF	X-ray fluorescence

1 Introduction

Correlated electrons in vanadium oxides are responsible for their unique structural, electrical, optical and magnetic properties. Their electronic band structures are affected by crystallographic structure, crystal field splitting and hybridization between O2p and V3d bands. There have been many experimental and theoretical studies of the band structure of the main vanadium oxides—V_2O_3, VO_2 and V_2O_5. The first experimental studies on band structure were based on optical spectroscopy that utilized absorption and reflection of light. Ceramic materials, single crystals and thin films were the subjects of these studies. Lately, new methods such as photoemission spectroscopy (PES), X-ray absorption or emission spectroscopy (XAS, XES) [1], X-ray reflectivity (XRR), X-ray fluorescence (XRF) [2], photoluminescence (PL) [3, 4], Raman scattering and scanning tunnelling microscopy (STM) [5] have been used.

Theoretical calculations used several quantum mechanics models such as the Hartree–Fock self-consistent field method based on one-electron approximation, the Hubbard–Mott model [6] introducing the effects of electron correlations on the Hamiltonian, Peierls mechanism [7, 8] involving electron–phonon interactions, or the density function theory (DFT) [9].

One of the most important parameters with regard to the properties of materials is the bandgap energy (E_g). Generally, the E_g of a semiconductor or an insulator has been found to decrease with increasing temperature. The variation of the fundamental E_g with temperature is very important for both basic science and technological applications.

2 Electronic structure

The theoretical basis of optical properties results from Maxwell's equations. From optical spectra, the complex dielectric function $\varepsilon(\omega)$ is derived [10]:

$$\varepsilon(\omega) = \varepsilon_1 - i\varepsilon_2 \tag{1}$$

✉ Krystyna Schneider
kryschna@agh.edu.pl

[1] Department of Electronics, Faculty of Computer Science, Electronics and Telecommunications, AGH University of Science and Technology, 30-059 Kraków, Poland

where ω is angular frequency of light ($\omega = 2\pi\nu$), ε_1 and ε_2 represent real and complex parts of ε, and i is the imaginary unit.

$$\varepsilon_1 = n^2 - \kappa^2 \tag{2}$$

and

$$\varepsilon_2 = 2n\kappa \tag{3}$$

where n and κ are real and imaginary parts of the refractive index.

Measurement of light absorption is one of the most important techniques used to determine the optical properties of solids. In absorption measurements, the intensity of light ($I(d)$) after it has travelled through a certain thickness of a material is compared with the incident intensity (I_o), thereby defining the absorption coefficient (α):

$$I(d) = I_o \exp[-\alpha(\omega)d] \tag{4}$$

The dependence of the absorption coefficient on frequency is shown in Fig. 1. Since $I(d)$ depends on the square of the field variables, it immediately follows that

$$\alpha(\omega) = 2\frac{\omega\,\kappa}{c} = 4\,\frac{\pi\kappa}{\lambda} \tag{5}$$

where the factor of 2 results from the definition of $\alpha(\omega)$ in terms of light intensity, which is proportional to the square of the optical fields. This expression entails that the absorption coefficient is proportional to ~ $\kappa(\omega)$, the imaginary part of the complex index of refraction (extinction coefficient), so that κ is usually associated with power loss.

It can be concluded from Eqs. (2), (3) and (5) that either set—(ε_1, ε_2) or (n, α)—represents the wavelength-dependent constants characterizing the optical properties of a studied solid. Many efforts have been devoted to the determination of the refractive index (n), but there is so far no universal approach. Several methods of calculating the refractive index of vanadium oxide [11–18] and other materials [19–23] have been proposed. Various assumptions were used in these methods, and the results are often subjective/debatable and ambiguous.

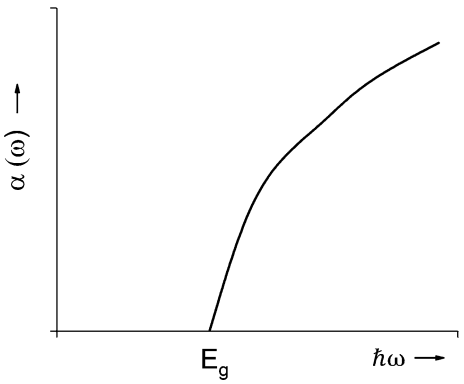

Fig. 1 Frequency dependence of the absorption coefficient (α) near the threshold for interband transition

2.1 Optical properties V_2O_5-literature survey

The electronic structure of vanadium pentoxide has been the subject of intensive studies [24–34]. Various theoretical calculations of V_2O_5 band structure include both semi-empirical and ab initio techniques.

Lambrecht et al. [24, 25] presented a calculation of the energy band structure using a tight-binding model in which the oxygen p-bands and vanadium d-bands were decoupled. They applied a perturbation approximation in order to obtain an effective Hamiltonian for the valence and conduction bands separately. The theoretically determined dispersion of the energy bands was verified by applying electrical transport properties. The valence band density of states was compared with XPS (X-ray photoelectron spectroscopy) and SXS (soft X-ray spectroscopy) data. The valence-to-conduction band transitions were compared with optical and electron energy loss (ELS) data. A satisfactory agreement between theoretical and experimental data was found [25].

Kempf et al. [26] reported on pseudo potential periodic Hartree–Fock calculations on a V_2O_5 crystal. The determined V-O bond lengths and stretching force constants were found to be in good agreement with experimental data. The estimated band structure and density of states remain in contrast with tight-binding calculations. There is no gap between the conductor and valence bands. According to the authors, vanadium pentoxide is partially ionic.

Bullett [27] determined the electronic structure of vanadium pentoxide using direct and non-empirical atomic orbital techniques. He postulated an indirect semiconducting energy gap of 2.6 eV.

Eyert and Höck [28] computed the band structure of bulk vanadium pentoxide using the density-functional theory (DFT) and local-density approximations (LDA). Its electronic properties were modified via strong hybridization between O 2p and crystal-field-split V3d orbitals. A strong deviation of VO_6 octahedra from the cubic coordination led to a narrow split-off conduction band.

The electronic structure of vanadium pentoxide is strongly connected with its anisotropy, which in turn is associated with its crystal structure. The atoms form double chains within planes that are separated by a van der Waals gap.

Kenny et al. [29] studied the optical absorption coefficients of V_2O_5 single crystals using incident polarized light with wavelengths in the range of 0.47–1.8 µm and unpolarized light with wavelengths from 1.5 to 7.5 µm. Fundamental absorption was observed at incident photon energies of

2.15, 2.22 and 2.17 eV for $E \| a$, $E \| b$ and $E \| c$, respectively. Some evidence for a direct forbidden transition mechanism with bandgaps of 2.36 and 2.34 eV was observed for $E \| a$ and $E \| c$, respectively. The most notable property of V_2O_5 is its ability to produce monolayers (or materials only several layers thick) [30]. Vanadium pentoxide is the second material known to exhibit such a property. The first one was graphite forming a single monolayer, known as graphene. Chakarbarti al. [31] determined the V_2O_5 monolayer band structure using *ab initio* density-functional theory (DFT). The obtained results are in excellent agreement with experimental crystallographic data as well as with other experimentally determined surface properties [32, 33].

Tolhurst et al. [34] studied a double-layered polymorph of V_2O_5 (named ε'-V_2O_5) using soft X-ray spectroscopic measurements and density-functional theory calculations. This polymorph has increased interlayer separation, which leads to a dramatic increase in the bandgap. Table 1 summarizes the representative literature data [28, 34–37] of the band gap and its temperature dependence.

Figure 2 shows the refractive index for vanadium pentoxide thin films as a function of wavelength [13, 38]. Parameter n decreases with wavelength. This dependence may be verified using the theoretical equation proposed by Cauchy [39]:

$$n(\lambda) = A + \frac{B}{\lambda^2} \tag{6}$$

where A and B are independent of λ. According to Fig. 3, the experimental points are consistent with the theory postulated by Cauchy.

The analysis of the dependence of the absorption coefficient on light frequency is very significant from the viewpoint of the semiconducting properties of vanadium oxide and its subsequent areas of application. Generally, the frequency dependence of the absorption coefficient ($\alpha(\omega)$) is rather different for various physical processes which occur during the interaction of light with the solid. In particular, the following cases can be observed [10]:

1. Free carrier absorption

(a) typical semiconductor

$$\alpha(\omega) \sim \omega^{-2} \tag{7}$$

(b) metals at low frequencies

$$\alpha(\omega) \sim \omega^{\frac{1}{2}} \tag{8}$$

Table 1 Bandgap (E_g) of V_2O_5 and its temperature dependence—dE_g/dT

E_g (eV)	DE_g/dT (eV/K)	Orientation	References
2.17	-6.1×10^{-4}	$E \| c$	[29], [35]
2.34			[29]
2.25			[36]
2.49 ($T \rightarrow 0$)			[37]
2.19		$E \| b$	[35]
2.363			[29]
2.22			[29]
2.23	7.3	$E \| a$	[36]
2.15			[29]
2.54 ($T \rightarrow 0$)	$-6.1 \cdot 10^{-4}$	$E \perp c$	[37]

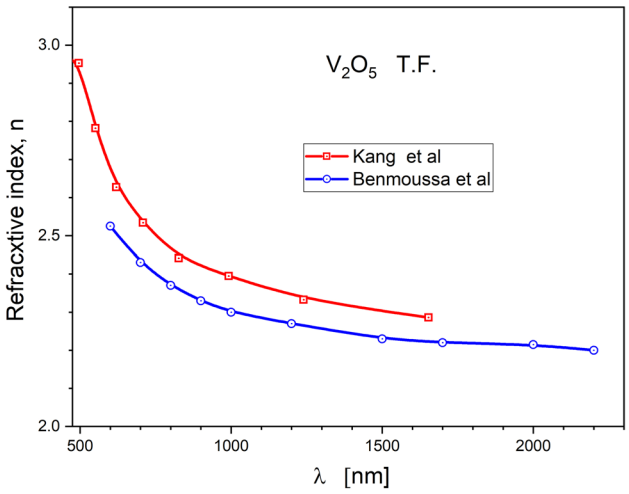

Fig. 2 Refractive index (n) determined for V_2O_5 thin films [13, 38]

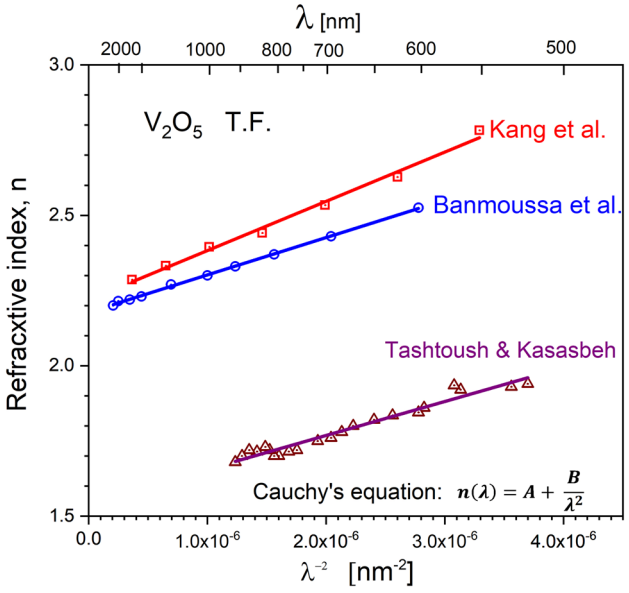

Fig. 3 Cauchy's plot of the refractive index (n) for V_2O_5 thin films [13, 16, 38]

2. Direct interband transition (conservation of crystal momentum)

(a) allowed transition

$$\alpha(\omega) \sim \frac{(\hbar\omega - E_g)^{\frac{1}{2}}}{\hbar\omega} \tag{9}$$

(b) forbidden transition

$$\alpha(\omega) \sim \frac{(\hbar\omega - E_g)^{\frac{3}{2}}}{\hbar\omega} \tag{10}$$

3. Indirect interband transition (change in crystal momentum)

(a) allowed transition

$$\alpha(\omega) \sim \frac{(\hbar\omega - E_g \pm \hbar\omega_{\text{phonon}})^2}{\hbar\omega} \tag{11}$$

(b) forbidden transition

$$\alpha(\omega) \sim \frac{(\hbar\omega - E_g \pm \hbar\omega_{\text{phonon}})^3}{\hbar\omega} \tag{12}$$

The $\hbar\omega_{\text{phonon}}$ factor is generally omitted in Eqs. (11) and (12) because of the fact that phonon energy is several times lower than the energy of electron transition. Equations (9)–(12), known as Tauc equations, are applied to determine the bandgap (E_g) of semiconductors.

Figure 4 shows the mechanisms of electron interband transition for direct and indirect semiconductors. A direct transition corresponds to the photon–electron interaction process in which the *k*-vector does not change. The crystal momentum of electrons and holes is the same in both the conduction band and the valence band. In an indirect transition photon, electron and phonon of the lattice take part. This process is accompanied by a change in the *k*-vector. The allowed transitions remain in agreement with particular selection rules, assuming a dipole model. On the other hand, if this model is not valid, the transition is called forbidden. More complex models can then be taken into account (involving, for instance, a magnetic dipole, electric quadrupole, etc.).

According to [29, 37], the edge is direct and forbidden. Diffuse reflectance spectra [40] give an E_g of 2.31 eV at room temperature, but the band edge has been determined to be direct and Mousavi et al. [41] observed that for V_2O_5 films prepared by means of spray pyrolysis E_g changes with the substrate temperature (T_{sub}). When T_{sub} increases, the E_g decreases gradually from 2.46 to 2.22 eV.

Kang et al. [5] studied the interband transition in a V_2O_5 film deposited via RF magnetron sputtering using absorption and photoluminescence spectral measurements. Transmission measurements indicate two distinct interband transitions, implying indirect and direct transitions.

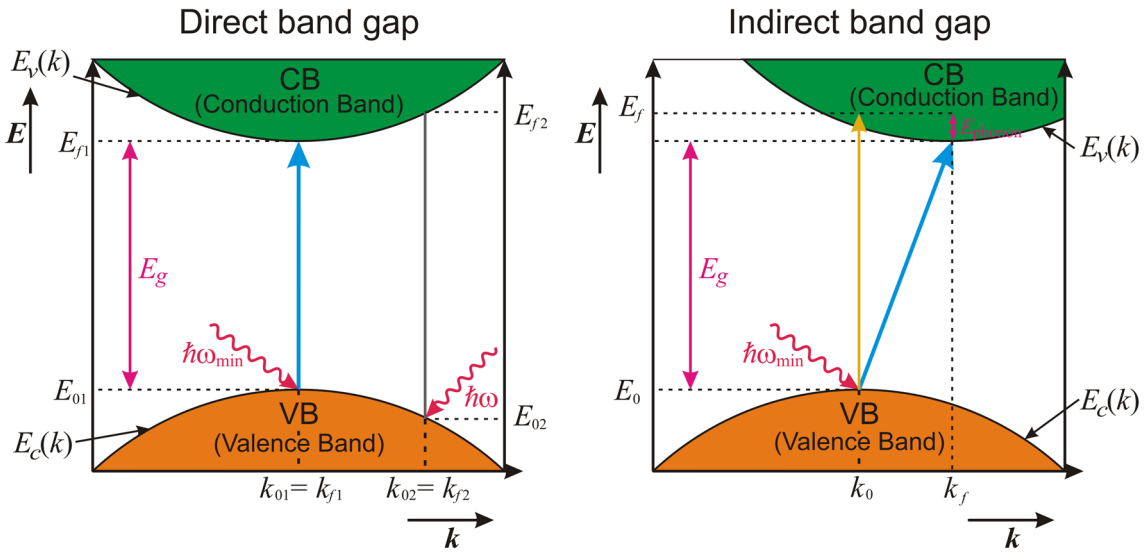

Fig. 4 Direct and indirect mechanisms of electron interband transition

Table 2 Deposition conditions for a series of vanadium oxide thin films and their properties

Deposition conditions	Series			
	1	2	3	4
Ar flow [cm^3/s]	6.3	6.7	6.7	6.7
O_2 flow (cm^3/s)	0.3	0.7	2.1	2.0
Input power (W)	290	280	290	220
RF voltage (U_{rf}) (V)	1150	1150	1150	1350
Ar/O_2 gas atmosphere pressure (Pa)	4.1×10^{-2}	4.3×10^{-2}	4.7×10^{-2}	4.6×10^{-2}
Deposition time (min)	240	240	240 360	240
Thickness (nm)	420 ± 49	421 ± 43	431 ± 28 630 ± 42	396 ± 30
Substrate	Corning, Ti, fused SiO_2	Corning, Ti, fused SiO_2,	Corning, Ti, fused SiO_2, BVT	Fused SiO_2
Substrate temperature (K)	298	298	298	298

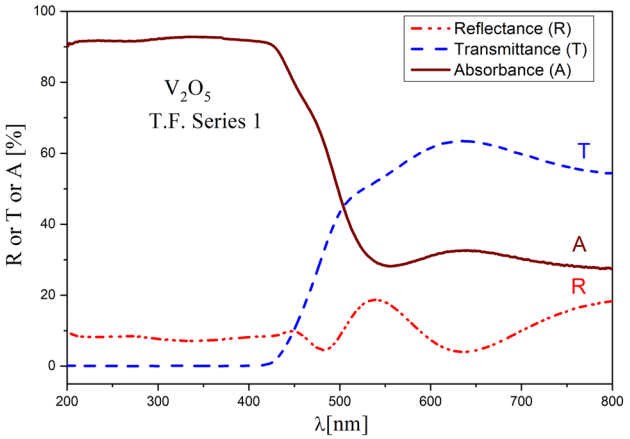

Fig. 5 Reflectance (R), transmittance (T) and absorbance (A) spectra recorded for a Series 1 V_2O_5 thin film

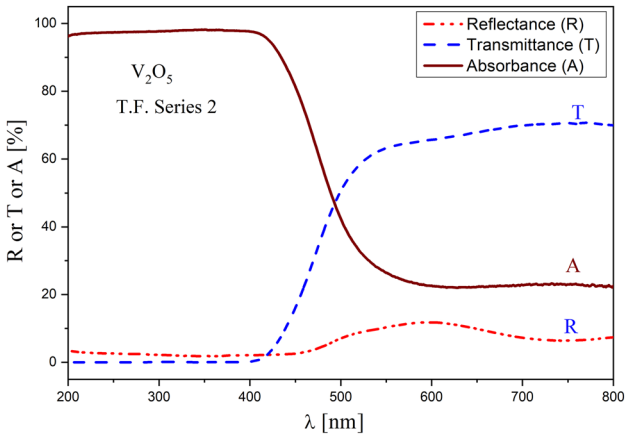

Fig. 6 Reflectance (R), transmittance (T) and absorbance (A) spectra recorded for a Series 2 V_2O_5 thin film

2.2 Optical properties of V_2O_5 thin films: experimental results

Vanadium pentoxide thin films were deposited by means of reactive radio frequency sputtering. Deposition conditions of the thin films and their properties such as structure, morphology were described in detail elsewhere [42]. Table 2 summarizes characterization of the films used in the studies.

Optical transmittance and reflectance spectra were measured over a wide wavelength range from 180 to 3200 nm with a Lambda 19 Perkin-Elmer double beam spectrophotometer equipped with a 150 mm integrating sphere. Thin films from Series 1, 2 and 3 were the subject of spectrophotometric studies. Each of Figs. 5, 6 and 7 shows the reflectance (R), transmittance (T) and absorbance (A) spectra recorded for one of the thin films. The transparency region of vanadium pentoxide is limited by the fundamental absorption edge at ca. 500 nm. The reflectance values vary in the

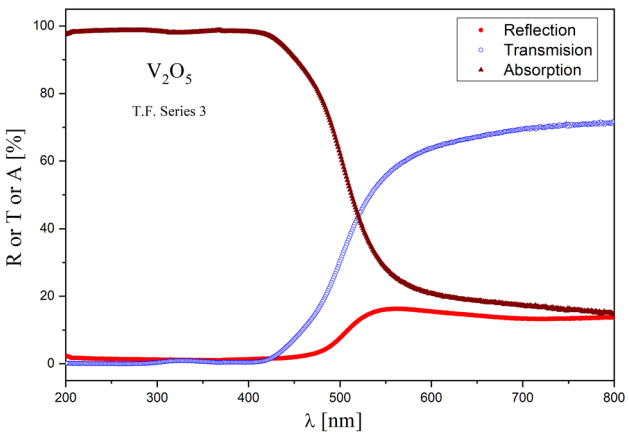

Fig. 7 Reflectance (R), transmittance (T) and absorbance (A) spectra recorded for a Series 3 V_2O_5 thin film

range of 10–20% for the Series 1 sample (mostly amorphous), in the range of ca. 0–10% for the Series 2 and 3 samples (crystalline). The observed non-monotonic plots of R, T and A may result from additional absorption bands due to the departure from stoichiometry [11, 12].

The absorption coefficient (α) and photon energy were determined from Figs. 5, 6 and 7 using the following equations:

$$\alpha = \frac{1}{d} \ln \frac{1-R}{T} \tag{13}$$

$$E_{\text{photon}}[eV] = \hbar\omega = \frac{1240}{\lambda[nm]} \tag{14}$$

where d represents film thickness.

One of the crucial parameters used to evaluate a semiconductor's properties is the bandgap (E_g). The bandgap of a semiconductor can be determined from experimentally measured transmittance T and reflectance R within the range of fundamental absorption using the following Tauc equation:

$$(\hbar\omega\alpha)^{\frac{1}{n}} = A\left(\hbar\omega - E_g\right) \tag{15}$$

where the A coefficient is constant and n, according to Eqs. (9)–(12), assumes values ½, 3/2, 2 and 3 for direct allowed (DA), direct forbidden, indirect allowed and indirect forbidden transitions, respectively.

Figures 8, 9, 10 and 11 illustrate the absorption coefficient data experimentally determined for the Series 2 thin film in the coordinate system of $(\alpha\hbar\omega)^{1/n}$ versus $\hbar\omega$ for n = ½, 3/2, 2 and 3, respectively.

The bandgap was determined by extrapolating the linear part of the best fit of $(\alpha\hbar\omega)^{1/n}$ vs. $\hbar\omega$ to $\alpha\hbar\omega = 0$. The values of E_g were obtained from the $\hbar\omega$ axis intercepts. Similar

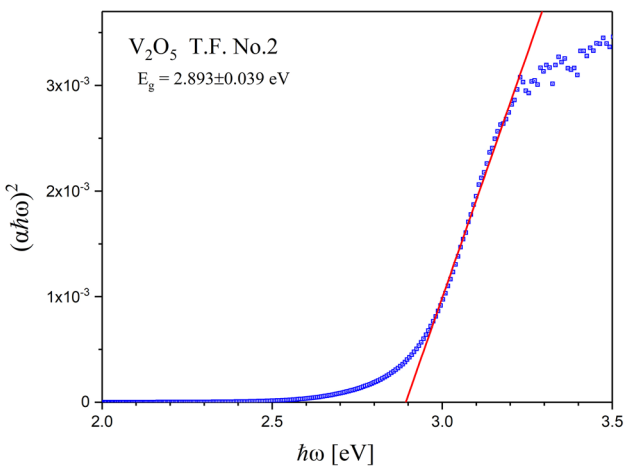

Fig. 8 Tauc plot (n = 2 – corresponding to a direct allowed transition) for a Series 2 V_2O_5 thin film

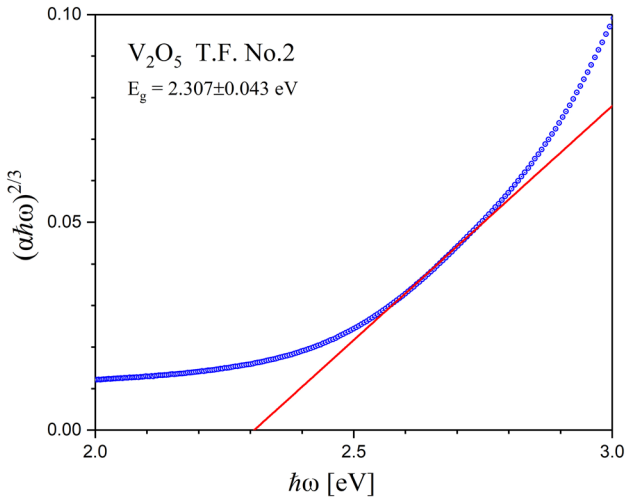

Fig. 9 Tauc plot (n = 3/2 – corresponding to a direct forbidden transition) for a Series 2 V_2O_5 thin film

plots were computed for the other two V_2O_5 samples: Series 1 and Series 3. The results are presented in Table 3.

The analysis of spectrometric results presented in Figs. 8, 9, 10 and 11 as well as in Table 3 suggests that V_2O_5 thin films undergo both direct and indirect transitions. However, it is not possible to decide which type of the electron interband transition is predominant in this case. Based on the following evidence,

- agreement with theoretical band calculations [24–26, 30],
- agreement with recent reports on single crystals [26, 43],
- agreement with recent experimental studies based not only on

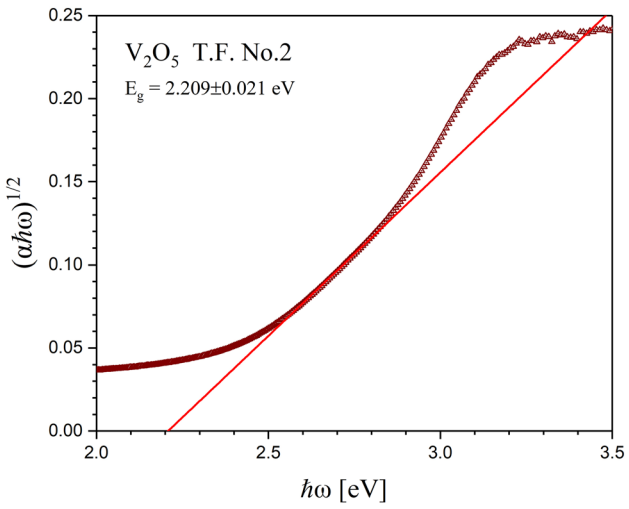

Fig. 10 Tauc plot (n = 2 – corresponding to an indirect allowed transition) for a Series 2 V_2O_5 thin film

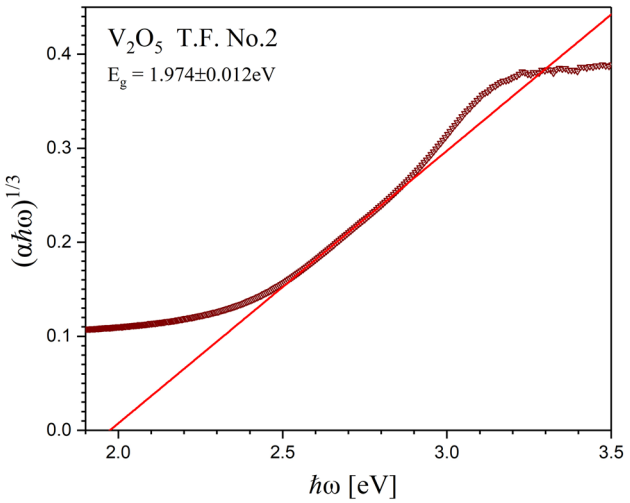

Fig. 11 Tauc plot ($n = 3$ − corresponding to an indirect forbidden transition) for a Series 2 V_2O_5 thin film

spectrophotometric measurements such as photoluminescence
and ellipsometry [17],

the direct allowed (DA) transition can be considered the most probable. The available literature on the bandgap of V_2O_5 thin film is vast. The impact of the following factors affecting the bandgap of films based on vanadium pentoxide has been studied:

- thin film deposition technique [44–46] (Table 3),
- anisotropy [28, 29, 31, 47]
- film thickness [34]
- substrate type [47]
- non-stoichiometry [13, 48, 49]
- UV irradiation [48]
- chemical composition [50]
- temperature [17, 43, 44, 47]
- morphology [13, 30, 34, 45]

The results are presented in Table 4.

Figure 12 illustrates the Tauc plots corresponding to $\hbar\omega$ energy between 2.97 and 3.23 eV. The best agreement with the theoretically predicted dependence is observed for the direct allowed (DA) transition. The results obtained by applying the least squares method are listed in Table 5.

2.3 Optical properties of V_2O_3

Based on papers [52–55], the most significant calculations were reported [56, 57]. The main controversy has been over the ordering of the components of the trigonally split t_{2g} band. Several band schemes have been suggested [58–60]. The V^{3+} ions in V_2O_3 have a $3d^2$ electronic configuration. These vanadium ions in the metallic phase (corundum) occupy two-thirds of the octahedral sites formed by oxygen anions. A trigonal distortion causes the splitting of the t_{2g} orbital into a non-degenerate a_{1g} and a doubly degenerate e^{II}_g orbital [61]. Castellani et al. [57] suggested the formation of a molecular bond between the a_{1g} orbitals of V–V pairs spread into a band. This model is consistent with many experimental results [62–65]. However, taking into account the fact that the c/a lattice parameter ratio is too high for a_{1g} to couple between two V cations, Ivanov [66] and Ezhov et al. [58] contradicted the postulated model of the molecular orbital. Shinna et al. [67] assumed a strong hybridization of the V pair.

The electronic properties of V_2O_3 are strongly dependent on oxygen stoichiometry.

A slight variation in oxygen concentration changes the effective mass [68, 69].

Table 3 Tauc plot results

Transition	Results		Series 1T.F.	Series 2 T.F.	Series 3 T.F.
Direct allowed	E_g (eV)		2.811 ± 0.065	2.893 ± 0.039	2.739 ± 0.089
	Linear regression	Number of points (n)	29	36	31
		Pearson correlation	0.9983	0.9978	0.9958
Direct forbidden	E_g (eV)		2.575 ± 0.105	2.307 ± 0.042	2.207 ± 0.051
	Linear regression	Number of points (n)	20	36	99
		Pearson correlation	0.9968	0.9988	0.9948
Indirect allowed	E_g (eV)		2.579 ± 0.064	2.209 ± 0.021	2.072 ± 0.030
	Linear regression	Number of points (n)	32	37	120
		Pearson correlation	0.9981	0.9997	0.9976
Indirect forbidden	E_g (eV)		1.969 ± 0.046	1.974 ± 0.012	1.782 ± 0.024
	Linear regression	Number of points (n)	30	52	107
		Pearson correlation	0.9988	0.9998	0.9985

Table 4 Summary of findings concerning the bandgap in vanadium pentoxide where DA, DF, IA and IF represent direct allowed, direct forbidden, indirect allowed and indirect forbidden transitions, respectively

Material	E_g (eV)	Electronic transition	Comments	Ref.
Single crystal	2.36 $\|\|a$; 2.34 $\|\|c$	DF	Anisotropy of E_g	[29]
Powder	2.31	DA		[47]
Single crystal	2.3	DA		[43]
Theoretical calculation	2.6	IA		[27]
Single crystal	Theoretical 1.9 experimental 2.0	IA	Ellipsometry	[51]
T.F. obtained via RF sputtering	2.15	IA	$d = 50$ nm	[28]
	$2.25^{p(O_2)} = 5\%$ $2.37^{p(O_2)} = 20\%$	DA	$d = 1000$ nm effect of $p(O_2)$ during film deposition	
T.F. obtained using electron beam	2.29–2.34	DF	Effect of UV irradiation (E_g increases after irradiation)	[48]
T.F. obtained using electron beam	$2.32^{303\ K}$ $1.98^{603\ K}$	DF	Effect of temperature deposition	[44]
Theoretical calculation	2.3^{DA}, 1.9^{IA} 2.3^{DA}, 2.1^{IA}	DA & IA	Bulk V_2O_5 Single-layer V_2O_5	[31]
Theoretical calculation	1.74			[30]
	1.67		Bulk V_2O_5	
	2.07		Single-layer V_2O_5	
T.F. obtained via magnetron sputtering	$2.67^{20\ K}$; $2.64^{300\ K}$	DA	$E_g = f(T)$	[17]
	$2.26^{20\ K}$; $2.16^{300\ K}$	IA		
T.F. obtained via spray pyrolysis	$1.98^{573\ K}$	DA	Effect of temperature deposition	[47]
	$2.05^{673\ K}$			
T.F. obtained via:		–	$E_g = f(p(O_2))$	[46]
E-beam evaporation	2.04–2.30	–	$E_g = f(T_{deposition})$	
	2.50^{RT}; $2.58^{673\ K}$	–		
Magnetron sput.	2.16–2.59	–		
CVD	2.15–2.20	–		
Sol-gel	2.42–2.49	–		
Laser beam	2.20–2.50			

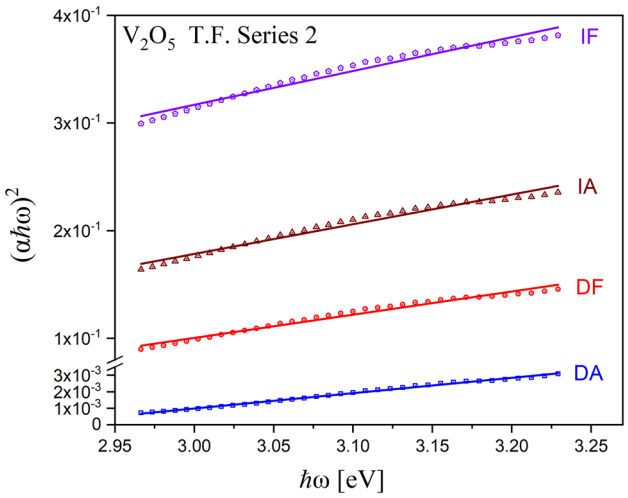

Fig. 12 Tauc plots for a Series 2 V_2O_5 thin film and the $\hbar\omega$ range of 2.97–3.23 eV

V_2O_3 is treated as the model system used to study the MIT in a correlated electron system (T_{MIT}= 160 K).

2.4 Optical properties of VO_2

The calculation of the electronic structure of VO_2 has been the subject of intensive research involving many models such as the cluster type [70, 71], tight-binding type [72–74], or augmented-plane-wave (APW) [75, 76], as well as energy band studies using Bloch functions in a linear combination of atomic orbitals [77].

Gavini et al. [78] determined the real (n) and imaginary (κ) parts of the refractive index. Studies of the absorption coefficient performed by Gavini et al. and Merenda et al. [79] revealed that the electronic structure at $E < 1.8$ eV can be attributed to d-d transitions with a threshold at 0.6 eV. At 1.82 eV, and the threshold for O2p–V3d transitions is observed, with peaks at 2.64 eV and 3.56 eV.

The temperature of MIT for bulk single-crystal VO_2 is 541 K [80]. Below T_{MIT}, VO_2 exhibits a monoclinic structure

Table 5 Results of calculations of the Tauc plot for the Series 2 V_2O_5 thin film and the ħω range of 2.97–3.23 eV, obtained using the least squares method

	Intercept	ΔIntercept	Slope	ΔSlope	$R_{corel.}$	E_g (eV)	ΔE_g (eV)
DA	0.02684	3.39E−04	0.00928	1.096E−04	0.9977	2.89	0.04
DF	0.54636	0.01733	0.21556	0.0056	0.98905	2.53	0.15
IA	0.64896	0.02417	0.27576	0.00781	0.98702	2.35	0.15
IF	0.62462	0.02984	0.31383	0.00964	0.98478	1.99	0.16

with the $P2_1/c$ space group in which the partially filled *d*-band is split into an unoccupied part pushed past the π^* band and the filled part of the *d*-band. Above the T_{MIT}, VO_2 transforms to a tetragonal (rutile) phase with the partially filled *d*-band located at the Fermi level and the material is metallic [81]. Jiang et al. [82] studied the optical properties of vanadium dioxide thin films deposited under different oxygen partial pressures via reactive magnetron sputtering. The bandgap decreased from 339.6 to 319.4 K. The near-infrared extinction coefficient (*k*) and optical conductivity increased with decreasing oxygen partial pressure.

3 Conclusions

The electronic structure of the three main vanadium oxides (V_2O_3, VO_2 and V_2O_5) was reviewed. The optical properties of vanadium pentoxide thin films were determined. It was found that the direct allowed (DA) transition is the most probable type observed in the case of the studied films.

Acknowledgements This work was supported by the National Science Centre of the Republic of Poland, under Grant No 2016/23/B/ST8/00163.

Open Access This article is licensed under a Creative Commons Attribution 4.0 International License, which permits use, sharing, adaptation, distribution and reproduction in any medium or format, as long as you give appropriate credit to the original author(s) and the source, provide a link to the Creative Commons licence, and indicate if changes were made. The images or other third party material in this article are included in the article's Creative Commons licence, unless indicated otherwise in a credit line to the material. If material is not included in the article's Creative Commons licence and your intended use is not permitted by statutory regulation or exceeds the permitted use, you will need to obtain permission directly from the copyright holder. To view a copy of this licence, visit http://creativecommons.org/licenses/by/4.0/.

References

1. N.B. Aetukuri, A.X. Gray, M. Drouard, M. Cossale, L. Gao, A.H. Reid, R. Kukreja, H. Ohldag, C.A. Jenkins, E. Arenholz, K.P. Roche, H.A. Durr, M.G. Samant, S.P. Parkin, Control of the metal-insulator transition in vanadium dioxide by moditying orbital occupancy. Nat. Phys. **9**(10), 661–666 (2013)
2. H.-P. Rust, J. Buisset, E.K. Schweizer, L. Cramer, High precision mechanical approach mechanism for a low temperature scanning tunnelling microscope. Rev. Sci. Instrum. **68**, 129 (1997)
3. N.F. Quackenbush, J.W. Tashman, J.A. Mundy, S. Sallis, H. Paik, R. Misra, J.A. Moyer, J.H. Guo, D.A. Fischer, J.C. Woicik, D.A. Muller, D.G. Schlom, L.F.J. Piper, Temperature dependence of the interband transition in a V_2O_5 film. AIP Adv. **3**, 052129 (2013)
4. N.F. Quackenbush, J.W. Tashman, J.A. Mundy, S. Sallis, H. Paik, R. Misra, J.A. Moyer, J.H. Guo, D.A. Fischer, J.C. Woicik, D.A. Muller, D.G. Schlom, L.F.J. Piper, Temperature dependence of the interband transition in a V_2O_5 film. Nano Lett. **13**(10), 4857–4861 (2013)
5. M. Kang, S.W. Kim, Y. Hwang, Y. Um, J.-W. Ryu, Temperature dependence of the interband transition in a V_2O_5film. AIP Adv. **3**, 052129 (2013)
6. J. Hubbard, Electron correlations in narrow energy bands. III. An improved solution. Proc. R. Soc. Lond. Ser. A **281**, 401–419 (1964)
7. R.E. Peierls, *Quantum Theory of Solid* (Oxford University, London, 1955)
8. S. Biermann, A. Poteryaev, A.I. Lichtenstein, A. Georges, Dynamical singlets and correlation-assisted peierls transition in VO_2. Phys. Rev. Lett. **94**, 026404 (2005)
9. P. Hohenberg, W. Kohn, Inhomogeneous electron gas. Phys. Rev. **136**, B864–B871 (1964)
10. M.S. Dresselhaus, *Solid State Physics. Part II Optical Properties of Solids* (Massachusetts Institute of Technology, Cambridge, 2001)
11. R.D. Bringans, The determination of the optical constants of thin films from measurements of normal incidence reflectance and transmittance. J. Phys. D Appl. Phys. **10**, 185501862 (1977)
12. G. Lévêque, Y. Villachon-Renard, Determination of optical constants of thin film from reflectance spectra. Appl. Phys. **29**, 3207–3212 (1990)
13. M. Benmoussa, E. Ibnouelghazi, A. Bennouna, E.L. Ameziane, Structural, electrical and optical properties of sputtered vanadium pentoxide thin films. Thin Solid Films **265**, 22–28 (1995)
14. J.J. Ruiz-Perez, Method for determining the optical constants of thin dielectric films with variable thickness using only their shrink reflection spectra. J. Phys. D Appl. Phys. **34**, 2489–2496 (2001)
15. A.K.S. Aquili, A. Maqsood, Determination of thickness, refractive index, and thickness irregularity for semiconductor thin films from transmission spectra. Appl. Opt. **41**, 218–224 (2002)
16. N.M. Tashtoush, O. Kasasbeh, Optical properties of vanadium pentoxide thin films prepared by thermal evaporation method. Jordan. J. Phys. **6**, 7–16 (2013)
17. M. Kang, S. Won Kim, Y. Hwang, Y. Um, J.-W. Ryu, Temperature dependence of the interband transition in a V_2O_5film. AIP Adv. **3**, 052129-1-05212.10 (2013)
18. S.J. Petel, V. Kheraj, Determination of refractive index and thickness of thin-film from reflectivity spectrum using genetic algorithm. AIP Conf. Proc. **1536**, 509 (2013). https://doi.org/10.1063/1.4810324
19. J. Szczyrbowski, A. Czapla, On the determination of optical constants of films. J. Phys. D Appl. Phys. **12**, 1737 (1979)

20. J. Szczyrbowski, K. Schmalzbauer, H. Hoffmann, Optical properties of rough thin films. Thin Solid Films **130**, 57–73 (1985)
21. J.M. Bennett, E. Polletier, G. Albrand, J.P. Borgogno, B. Lazarides, C.K. Carniglia, R.A. Schmell, T.H. Allen, T. Tuttle-Hart, K.H. Guenther, A. Saxer, Comparison of the properties of titanium dioxide films prepared by various techniques. Appl. Opt. **28**, 3303–3317 (1989)
22. A. Brudnik, H. Czternastek, K. Zakrzewska, M. Jachimowski, Plasma-emission-controlled d.c. magnetron sputtering of TiO_{2-x} thin films. Thin Solid Films **199**, 45–58 (1991)
23. T. Pisarkiewicz, Reflection spectrum for a thin film with non-uniform thickness. J. Phys. D Appl. Phys. **27**, 160–164 (1994)
24. W. Lambrecht, B. Djafari-Rouhani, M. Lannoo, J. Vennik, The energy band structure of V_2O_5. I. Theoretical approach and band calculations. J. Phys. C: Solid State Phys. **13**, 2485–2501 (1980)
25. W. Lambrecht, B. Djafari-Rouhani, M. Lannoo, P. Clauws, L. Fiermans, J. Vennik, The energy band structure of V_2O_5. II. Analysis of the theoretical results and comparison with experimental data. J. Phys. C: Solid State Phys. **13**, 2503–2517 (1980)
26. J.Y. Kempf, B. Silvi, A. Dietrich, C.R.A. Catlow, Theoretical investigations of the electronic properties of vanadium oxides. 1. Pseudopotential periodic Hartree-Fock study of vanadium pentoxide crystal. Chem. Mater. **5**, 641 (1993)
27. D.W. Bullett, The energy band structure of V_2O_5: a simple theoretical approach. J. Phys. C: Solid State Phys. **13**, L595–L599 (1980)
28. V. Eyert, K.-H. Höck, Electronic structure of V_2O_5: role of octahedral deformations. Phys. Rev. B **57**, 12727–12737 (1998)
29. N. Kenny, C.R. Kennewurf, D.H. Whitmore, Optical absorption coefficients of vanadium pentoxide single crystals. J. Phys. Chem. Solids **27**, 1237–1246 (1966)
30. G. Stewart, *Electronic Band Structure of Bulk and Monolayer* V_2O_5 (Case Western Reserve University, Cleveland, 2012), pp. 1–26
31. A. Chakarbarti, K. Hermann, R. Druzinic, M. Witko, F. Wagner, M. Petersen, Geometric and electronic structure of vanadium pentoxide: a density functional bulk and surface study. Phys. Rev. B **16**, 10583–10590 (1999)
32. R.A. Goschke, K. Vey, M. Maier, U. Walter, E. Göring, M. Klemm, S. Horn, Tip induces changes of atomic scale images of the vanadium pentoxide surface. Surf. Sci. **348**, 305–310 (1996)
33. A.D. Costa, C. Mathieu, Y. Barbaux, H. Poelman, G. Dalmai-Vennik, L. Lichtman, Observation of the V_2O_5 (001) surface using ambient atomic force microscopy. Surf. Sci. **370**, 339–344 (1997)
34. T.M. Tolhurst, B. Leedahl, J.L. Andrews, S. Banerjee, A. Moewes, The electronic structure of ε'-V_2O_5: an expanded band gap in a double-layered polymorph with increased interlayer separation. J. Mater. Chem. A **45**, 23694–23703 (2017)
35. D.S. Volzhenski, V.A. Grin, V.G. Savitskii, Kristallografiya **21**, 1238 (1976)
36. Z. Luo, Z. Wu, X. Xu, M. Du, T. Wang, Y. Jiang, Impact of substrate temperature on the microstructure, electrical and optical properties of sputtered nanoparticle V_2O_5 thin films. Vacuum **85**, 145–150 (2010)
37. Z. Bodo, I. Hevesi, Optical absorption near absorption edge in V_2O_5 single crystal. Phys. Stat. Solidi **20**, K45 (1967)
38. M. Kang, I. Kim, S. Kim, H.Y. Park, Metal-insulator transition without structural phase transition in V_2O_5 film. Appl. Phys. Lett. **98**, 131907–131916 (2011)
39. F.A. Jenkins, H.E. White, *Fundamentals of Optics*, 4th edn. (McGraw-Hill Inc, Singapore, 1981)
40. B. Karvaly, I. Hevesi, Investigations of diffuse reflectance sopectra of V_2O_5 powder. Z. Naturforsch. Teil A **26**, 245–249 (1971)
41. M. Mousavi, A. Kompany, N. Shahtahmasebi, M.M. Bagheri-Mohagheghi, Study of structural, electrical and optical properties of vanadium oxide condensed films deposited by spray pyrolysis technique. Adv. Manuf. **1**, 320–328 (2013)
42. K. Schneider, Vanadium oxides—properties and applications. Part IV, this issue
43. M.M. Margoni, S. Mathuri, K. Ramamurthi, R. Ramesh Babu, K. Sethuraman, Sprayed vanadium pentoxide thin films: influence of substrate temperature and role of HNO_3on the structural, optical morphological and electrical properties. Appl. Surf. Sci. **418**, 280–290 (2017)
44. C.V. Ramana, O.M. Hussain, B. Srinivasulu Naidu, P.J. Reddy, Spectroscopic characterization of electron-beam evaporated V_2O_5 thin films. Thin Solid Films **305**, 219–226 (1997)
45. E.E. Chain, Optical properties of vanadium dioxide and vanadium pentoxide thin films. Appl. Opt. **30**, 2782–2787 (1991)
46. S. Beke, A review of the growth of V_2O_5 films from 1885 to 2010. Thin Solid Films **519**(2011), 1763–1771 (2011)
47. J. Meyer, K. Zilberberg, T. Riedl, A. Khan, Electronic structure of vanadium pentoxide: an efficient hole injector for organic electronic materials. J. Appl. Phys. **110**(033710), 1–5 (2011)
48. S. Krishnakumar, C.S. Menon, Optical and electrical properties of vanadium pentoxide thin film. Phys. Stat. Sol. (a) **153**, 439–444 (1996)
49. M.J. Scepanovic, M. Grujić-Brojčin, Z. Dohčević-Mitrović, K. Vojisavljevic, Z. Popovic, The effects of nonstoichiomnetry on optical properties of oxide nanopowders. Acta Phys. Polon. Ser. a **112**, 1013 (2007)
50. D. Souri, K. Shomalian, Band gap determination by absorption spectrum fitting method (ASF) and structural properties of different compositions of $(60\text{-}x)V_2O_{5.4}0TeO_{2.x}Sb_2O_3$ glasses. J. Non-Cryst. Solids **355**, 1597–1601 (2009)
51. J.C. Parker, D.J. Lam, Y.-N. Xu, W.Y. Ching, Optical properties of vanadium pentoxide determined from elipsometry and band-structure calculations. Phys. Rev. B **42**, 5289–5293 (1990)
52. I. Nebenzahl, M. Weger, Band structure of the 3d-t_{2g} sub-shell of V_2O_3 and Ti_2O_3 in the tight-binding approximation. Philos. Mag. **24**, 1119 (1971)
53. M. Weger, Application of the excitonic model to the metal-insulator transition of a simple band model. Philos. Mag. **24**, 1095 (1971)
54. J. Ashkenazi, M. Weger, A model for the metal-to-insulator transition in V_2O_3. Adv. Phys. **22**, 207–261 (1973)
55. J. Ashkenazi, T. Chuchem, Band structure of V_2O_3 and Ti_2O_3. Philos. Mag. **32**, 763 (1975)
56. J. Ashkenazi, M. Weger, The effect of band structure and electron-electron interactions on the metal-insulator transitions in Ti_2O_3 and V_2O_3. J. Phys. **37**, C4-189-C4-180 (1976)
57. C. Castellani, C.R. Natoli, J. Ranninger, Magnetic structure of V_2O_3 in the insulating phase. Phys. Rev. B **18**, 4945–4967 (1978)
58. S. Yu Ezhov, V.I. Ansimov, D.I. Khomski, G.A. Sawatzky, Orbital occupation, local spin and exchange interactions in V_2O_3. Phys. Rev. Lett. **83**, 4136–4139 (1999)
59. J.M. Honig, L.L. Van Zandt, R.D. Board, H.E. Weaver, Study of $V_2O_3$by X-ray photoelectron spectroscopy. Phys. Rev. B **6**, 323 (1972)
60. P. Shuker, Y. Yacoby, Differential reflectance spectra and band structure of V_2O_3. Phys. Rev. B **14**, 2211 (1976)
61. J.W. Taylor, T.J. Smith, K.H. Andersen, H. Capellman, R.K. Kremer, A. Simon, K.-U. Neumann, K.R.A. Ziebeck, Spin-spin correlations in the insulating and metallic phases of the Mott system V_2O_3. Eur. Phys. J. B Condens. Matter Complex Syst. **12**, 199–207 (1999)
62. L. Paolasini, C. Vettier, F. De Bergevin, F. Yakhou, D. Mannix, W. Neubeck, A. Stunault, M. Altarelli, M. Fabrizio, P.A. Metcalf, J.M. Honig, Direct observation of orbital ordering in

V_2O_3 by X-ray scattering technique. Phys. B **281–282**, 485–486 (2000)
63. M. Fabrizio, M. Altarelli, M. Benfatto, X-ray resonant scattering as a direct probe of orbital ordering in transition-metal oxides. Phys. Rev. Lett. **80**, 3400 (1998)
64. L. Paolasini, C. Vettier, F. De Bergevin, F. Yakhou, D. Mannix, A. Stunault, W. Neubeck, M. Altarelli, M. Fabrizio, P.A. Metcalf, J.M. Honig, Orbital occupancy order in V_2O_3: resonant X-ray scattering results. Phys. Rev. Lett. **82**, 4719–4722 (1999)
65. W. Bao, C. Broholm, G. Aeppli, P. Dai, J.M. Honig, P. Metcalf, Dramatic switching of magnetic exchange in a classic transition metal oxides: evidence for orbital ordering. Phys. Rev. Lett. **78**, 507–510 (1997)
66. V.A. Ivanov, The tight-binding approach to the corundum-structure d compounds. J. Phys.: Condens. Matter **6**, 2065–2076 (1994)
67. R. Shiina, F. Mila, F.-C. Zhang, T.M. Rice, Phys. Rev. B **63**, 144422 (2001)
68. C.A. Carter, T.F. Rosenbaum, P. Metcalf, Mass enhancement and magnetic order at the Mott-Hubard transition. Phys. Rev. B **48**, 16841–16844 (1993)
69. J. Trastoy, Y. Kaicheim, J. del Valle, I. Valmanski, I.K. Schuller, Electronic materials. J. Mater. Sci. **53**, 9131–9137 (2018)
70. N.I. Lazukova, V.A. Gubanov, Metal-insulator phase transition in VO_2. Solid State Commun. **20**, C4–C59 (1976)
71. C. Sommers, R. de Groot, D. Kaplan, A. Zylberstejn, Soft X-ray absorption spectroscopy of vanadium oxides. J. Phys. Lett. **36**, L-157 (1975)
72. T.K. Mitra, S. Chatterjee, G.J. Hyland, A L.C.O.A.O. approach to the band structure of rutile VO_2. Phys. Lett. A **37**, 221–222 (1971)
73. T.K. Mitra, S. Chatterjee, G.J. Hyland, Amethod for obtaining parametrized bands of rutile VO_2. Can. J. Phys. **51**, 352–365 (1973)
74. T. Altanham, G.J. Hyland, One-electron dispersion relations in metallic VO_2. Phys. Lett. A **61**, 426–428 (1977)
75. E. Caruthers, L. Kleinman, H.I. Zhang, Energy bands of metallic VO_2. Phys. Rev. B **7**, 3753–3760 (1973)
76. E. Caruthers, L. Kleinman, Energy bands of semiconducting VO_2. Phys. Rev. B **7**, 3760–3766 (1973)
77. M. Gupta, A.J. Freeman, D.E. Elilis, Electronic structure and lattice stability of metallic VO_2. Phys. Rev. B. **16**, 3338–3351 (1977)
78. A. Gavini, C.C.Y. Kwan, Optical properties of semiconducting VO_2films. Phys. Rev. B **3**, 3138–3143 (1972)
79. P. Merenda, D. Kaplan, C. Sommers, Nearband gap optical absorption on semiconducting VO_2. J. Phys. Colloques **37**, C4-59-C4-62 (1976)
80. F.I. Morin, Oxides which show a metal-to-insulator transition at the Neel temperature. Phys. Rev. Lett. **3**, 34–36 (1959)
81. T.C. Koethe, Z. Hu, M.W. Haverkort, C. Schüβler-Langeheine, F. Venturini, N.B. Brookes, O. Tjernberg, W. Reichelt, H.H. Hsieh, H.-J. Lin, C.T. Chen, L.H. Tjeng, Transfer of spectral weight and symmetry across the metal-insulator transition in VO_2. Phys. Rev. Lett. **97**, 116402 (2006)
82. M. Jiang, Y. Li, S. Li, H. Zhou, X. Cao, S. Bao, Y. Gao, H. Luo, P. Jin, Room temperature optical constants and band gap evolution of phase pure M_1-VO_2 thin films deposited at different oxygen partial pressure by reactive magnetron sputtering. J. Nanomater. **2014**, 183954 (2014)

Publisher's Note Springer Nature remains neutral with regard to jurisdictional claims in published maps and institutional affiliations.